

Polarized Internal Reflectance Spectroscopic Studies of Oriented Poly(ethylene terephthalate)

E. A. LOFGREN and S. A. JABARIN

Polymer Institute, College of Engineering, The University of Toledo, Toledo, Ohio 43606-3390

SYNOPSIS

Polarized internal reflectance spectroscopy (IRS) has been used to evaluate molecular orientation and crystallinity of poly(ethylene terephthalate) film surfaces. Measurements were taken using samples stretched in both uniaxial and biaxial modes. All bands of interest were normalized with a reference band near 1410 cm^{-1} , resulting from phenylene ring vibrations. Normalization was performed in order to overcome problems with sample contact and effective thickness. Results obtained using bands representing *trans* and *gauche* rotational isomers, present, respectively, at 1340 and 1370 cm^{-1} , have been related to data acquired using density and birefringence techniques. The polarized IRS technique discussed is well suited for investigations of polymer orientation and crystallinity, since it avoids limitations related to sample thickness and clarity imposed by polarized transmission infrared spectroscopy. Parameters such as orientation functions, attenuation indices, dichroic ratios, and structural factors have been determined from data collected in each of the three spatial directions. Results are correlated with corresponding density, birefringence, and refractive index values and are found to give good agreement with these methods. © 1994 John Wiley & Sons, Inc.

INTRODUCTION

The structure and orientation of poly(ethylene terephthalate) (PET) have been studied extensively by infrared absorption spectroscopy.¹⁻¹⁷ The spectrum of PET is known to be sensitive to changes in polymer crystallinity, molecular conformation, and molecular orientation. Early interpretation assigned the *trans* conformational structure to molecular sequences in the crystalline phase of PET and the *gauche* conformation to sequences in the amorphous phase. Additional investigations revealed, however, that the amorphous phase contains equilibrium amounts of *trans* and *gauche* structures.^{1,8,15} Overall, an increase in crystallinity has been correlated with a decrease in the amount of PET with ethylene glycol units in the *gauche*, or relaxed form, and an increase in the number of ethylene glycol units in the *trans*, or extended conformation.^{5,8}

The study of transmission spectra of PET requires that samples be very thin ($\sim 0.05\text{ mm}$) to

prevent total absorption of most bands. Since many samples cannot easily meet this requirement, alternative spectral techniques, utilizing samples in contact with multiple internal reflection elements, have been found useful.¹⁸⁻²³

In addition to permitting measurement of thicker and more opaque samples, internal reflection spectroscopy (IRS) eliminates the complex tilting experiments^{1,16,17} required to obtain transmission values in the normal, or thickness, direction of film samples. Measurements in the normal direction are possible with IRS because the evanescent field has vectors present in all spatial orientation at the thin surface layer next to the internal reflectance element. Values can, therefore, be obtained in the machine and transverse directions (as most often reported for transmission spectroscopy) as well as in the normal orientation direction. Flournoy and Schaffers¹⁸ first derived equations for quantitative IRS measurements of molecular orientation in the three spatial directions. Their work permitted calculation of spatial attenuation indices from measured reflectivities obtained using polarized energy. These directional orientation relationships were

then used to establish macromolecular similarities between surface and bulk properties of oriented polymer films.^{7,19,22,23}

Schmidt¹ was among the first investigators to study orientation of stretched PET using polarized transmission infrared spectroscopy. He found bands at 973 cm⁻¹ (*trans*), 896 cm⁻¹ (*trans*), and 848 cm⁻¹ (*gauche*) to be sensitive to changes in molecular orientation as well as to conformation. This work also utilized conformationally insensitive bands at 875 and 795 cm⁻¹ to correct for variations in sample thickness. These reference bands, however, were sensitive to orientation effects, which were corrected by normalized absorbance values obtained in the three spatial directions [$\frac{1}{3}(A_x + A_y + A_z)$] to obtain a structural factor (A_0), stripped of orientation effects. Using this technique, absorbance values in each individual orientation direction for the band of interest could be ratioed with A_0 to give measurements of the relative degree of orientation. In addition, A_0 could be obtained for the band of interest and ratioed with A_0 for the reference band to obtain structural factors (with orientation effects removed) at conformationally sensitive wavenumbers.

The above calculations, although effective for transmission spectra, cannot be directly applied to IRS techniques. With transmission spectroscopy, values of equivalent intensity in the machine and transverse directions can be obtained simply by rotating the polarization 90°. This is not possible with IRS, because the effective sample thickness is different when using the transverse electric (TE) vs. the transverse magnetic (TM) waves.²² This problem could be avoided by measuring both sample orientation directions with the TE wave, but then sample unclamping and reclamping to the IRS element would be required. Sung et al.^{11,12} developed a double-cut internal reflectance element that permits measurements to be obtained in machine and transverse directions without removing and reclamping the samples. Mirabella and Karrick,²² however, contended that the contact area may vary as a result of orientation and crystalline structure even when sample and reflectance element contact is not broken.

Problems with effective thickness and optical contact discussed above may be minimized by normalizing bands of interest with reference bands known to be insensitive to sample orientation and conformation.^{13,22,23} The reference band should also be close to the frequency of the bands of interest to ensure equivalent evanescent depths.¹³ Walls¹³ identified a ring vibrational band near 1410 cm⁻¹

for use in the analyses of surface composition and orientation of PET. Using samples stretched uniaxially up to four times their original lengths, he measured absorption values for various bands with both TE and TM excitations. Samples were positioned with either their machine or transverse directions parallel to the TE excitation. In each case, addition values were taken with TM excitations. Ratios of TE to TM absorption remained constant at 1410 cm⁻¹, regardless of sample position or draw ratio. These results, obtained with four experiential geometries, indicate that the 1410 cm⁻¹ band is not sensitive to changes in orientation or conformation and is therefore a good choice for use as a normalizing reference band. Because of their close proximity to the 1410 cm⁻¹ reference band, *gauche* and *trans* bands at 1370 and 1340 cm⁻¹, respectively, were chosen to monitor sample changes resulting from orientation.

The following studies have utilized the reference band at 1410 cm⁻¹ as a normalizing band for investigations of molecular orientation using IRS. Absorption values have been recorded at a variety of vibrational bands, sensitive to changes in conformation and/or orientation, using samples prepared under conditions of both uniaxial and biaxial extension. Equations derived by Flournoy and Schaffers¹⁸ have been employed at selected wavenumbers to determine molecular orientation in the three spatial directions. These and additional orientational effects have been related to changes in density and birefringence.

EXPERIMENTAL

Stretched samples were prepared from extruded sheets of substantially amorphous Goodyear 7202A PET. Sheets had an initial thickness of about 0.5 mm (20 mil), an inherent viscosity of 0.66, and contained ~ 1.3 wt % diethylene glycol. A Long Extensional Tester (LET) was used to stretch all samples at a temperature of 90° and a speed of 15.2 cm/s. Uniaxial or one-directionally stretched samples were constrained in the transverse direction and stretched up to 3.8 times their original lengths in the machine direction. Equal biaxially stretched samples were stretched in both directions simultaneously at the same rate. Unequal biaxially stretched samples were simultaneously stretched at 15.2 cm/s in both directions up to the shortest stretch direction. Stretching was then continued sequentially, at the same rate, up to the longest stretch direction.

Samples to be used for IRS measurements were cut from the stretched sheets as rectangles approximately 10 by 48 mm. For sheets prepared at each stretching condition, two pairs of samples were cut. One pair of samples was cut with the long dimension parallel to the longest stretching direction of the sheet. A second set was cut perpendicular to the first pair of samples, with the long dimension parallel to the shortest stretching direction of the sheet. Care was taken to ensure that the sample directions were aligned with the edges of the LET stretched sheets, while cutting them from central portions of each sheet to avoid "edge"-related distortions.

Each pair of cut samples was then positioned, one on each side of a $50 \times 20 \times 2$ mm thallium bromide-iodide (KRS-5) 45° , reflectance element, mounted in a Harrick internal reflectance accessory. The accessory was placed in a Harrick TMP-V twin parallel mirror reflectance attachment. Spectra, obtained from 256 scans, were recorded using a Perkin-Elmer Model 1600 FTIR spectrophotometer, equipped with a wire grid polarizer. Measurements were performed with the electric vector of the transmitted, plane-polarized radiation, parallel to the entrance slit of the spectrophotometer. Additional measurements were performed with the polarizer rotated 90° . All spectra were recorded at 4 cm^{-1} resolution. Specified band intensities were ratioed with the 1410 cm^{-1} reference band shown by Walls¹³ to be insensitive to orientation as well as to sample conformation. This was done to account for variations in sample contact with the reflectance element and effective sample thickness. Peak heights were taken using standard Perkin-Elmer software.

Density was determined at 25°C according to ASTM procedure D 1505-85. The density gradient column was prepared from aqueous calcium nitrate solutions and calibrated with glass beads of known densities. Accuracy was within $\pm 0.0003 \text{ g/cm}^3$.

Birefringence was calculated from the refractive indices measured in the three principal directions using an Abbe-3L refractometer equipped with a polarizing eyepiece; according to the method of Okajima et al.²⁴ as described by Schael.²⁵ The temperature was maintained at $25 \pm 0.1^\circ\text{C}$.

RESULTS AND DISCUSSION

It is known that under certain stretching conditions PET will undergo orientation and strain-induced crystallization.²⁶⁻²⁸ Many changes in physical and material properties have been related to these phenomena.²⁶⁻³⁰ Previous workers have investigated ef-

fects of crystallization and orientation upon specific sensitive infrared absorption bands. Spectra have been recorded using polarized and nonpolarized energy with transmission and multiple internal reflectance techniques. Because of its complexity, however, the majority of reported work has dealt primarily with uniaxially stretched samples. Current work utilizes a polarized IRS technique to monitor changes in molecular orientation resulting from biaxial as well as uniaxial orientation.

The accuracy and reproducibility of data obtained using IRS techniques are extremely sensitive to sampling variations, resulting from differences in contact between the sample and the reflectance element (optical contact) as well as to changes in signal penetration (effective sample thickness). To compensate for these problems, absorbance bands of interest are often normalized with reference bands, known to be insensitive to changes in sample conformation and orientation. Walls¹³ presented extensive experimental evidence to establish the reliability of the ring vibration band near 1410 cm^{-1} for this purpose. Absorbance values, obtained for samples included in this orientation study, have therefore been normalized with the 1410 cm^{-1} reference band.

Absorbance data were recorded using four different combinations of excitation energy and sample position for each orientation condition. Measurements were taken with transverse electric (TE) excitation parallel to the lesser stretched direction of the sample to give transverse direction (TD) absorption values. In this case, the greatest sample stretching direction (MD) was parallel to the long direction of the KRS-5 reflectance element, making the TE wave parallel to the electric dipole moment change, coupled to the group vibration under consideration²² in the TD. With the sample position unchanged, the polarizer was rotated 90° to provide transverse magnetic (TM) excitation data. Absorption values measured with TM waves then included components from both the major stretching direction or machine direction (MD) and the thickness or normal direction (ND) orientations. Additional values were obtained by repeating the above procedure with sample materials cut perpendicular to the previous sample. In this case, TE excitation yielded MD absorption and TM waves gave combined values for TD and ND absorption.

Absorbance values, obtained in the above manner, were measured at several of the infrared bands most commonly utilized for monitoring changes in crystallinity and orientation of PET. Values recorded for each band were normalized with the 1410 cm^{-1}

reference band. Tables I and II show normalized absorption values for each of the four sample vs. polarizer arrangements. Data are given at a variety of wavenumbers for a broad range of uniaxial and biaxial sample extension ratios.

Structure and orientation sensitive *trans* bands at 1340, 973, and 848 cm^{-1} are characteristic of the extended form of the ethylene glycol linkages of PET.^{1,2,13} These rotational isomers are believed to be present in both crystalline and amorphous regions of the polymer. Schmidt¹ proposed a method for determining levels of *trans* content present in the amorphous phase of PET, as separate from that in the crystalline phase. His work, which related *trans* content to material density, established values for equilibrium *trans* content in totally amorphous as well as 100% crystalline polymer.

Normalized *trans* intensity values are shown on Tables I and II for samples stretched to various extension ratios in the uniaxial and biaxial modes. If polymer orientation has occurred during stretching, *trans* intensity, measured in the direction of greatest orientation, would be expected to increase. This increase would result from higher levels of crystallinity and therefore greater crystalline *trans* content, as well as from molecular orientation in the amorphous phase and its accompanying increased amorphous *trans* content.

Data obtained at all three *trans* wavenumbers show larger values in the greatest stretching direction (MD) as extension ratios are increased up to moderate levels. At higher extension ratios, however, values taken at 973 and 848 cm^{-1} do not continue to increase at the same rate. At very high levels of extension, the wavenumbers at which these bands appear are shifted significantly and the peaks are extremely distorted in shape. Absorbance values recorded for the *trans* band at 1340 cm^{-1} do not exhibit problems of this nature. As sample extension ratios increase, *trans* contents as indicated by this band also continue to increase. Peaks recorded at 1340 cm^{-1} appear without being distorted or shifted, regardless of sample extension ratio. An additional advantage gained by using the *trans* band at 1340 cm^{-1} is its close proximity to the 1410 cm^{-1} reference band.¹³ Since these bands occur at very similar wavenumbers, measurement complications resulting from large differences in signal penetration and effective sample thickness between the *trans* and reference bands are eliminated.

Changes in *trans* contents, resulting from molecular orientation, can be observed most easily for samples stretched uniaxially or in one direction (MD) while being constrained in the other direction

(TD). Figure 1 shows changes, in the normalized 1340 cm^{-1} *trans* band, that result from stretching unoriented amorphous PET up to 3.8 times the original sample length. In this figure, *trans* values are plotted as a function of planar extension, which is the product of sample extension ratios in the greater and lesser stretching directions (MD \times TD). Measurements taken in the direction of stretching (MD) are designated by filled circles (\bullet) while those in the constrained, unstretched direction (TD) are indicated with open circles (\circ). These data were recorded with the transverse electric (TE) wave parallel to the direction indicated in each case. It can be seen that *trans* content in the direction of stretching increases with increased extension ratio. The magnitude of this change increases after an extension ratio of 1 \times 2 has been exceeded. Values measured in the constrained direction (TD) show little change as a result of increased planar extension. These results are similar to previously reported mechanical property results^{1,2,30} in which properties such as yield stress increased in the MD but remained relatively unchanged in the TD.

Changes in *gauche* content, as a function of uniaxial planar extension, are shown in Figure 2. Normalized absorption values show a steady decline, as polymer segments undergo rotation and conversion from *gauche* to *trans* conformations. In this case, no consistent differences are seen between measurements performed with the TE wave parallel to the material's MD or TD. This behavior is as expected, since material in the *gauche* or relaxed state is not sensitive to orientation direction. The process of molecular orientation converts material from the *gauche* to the *trans* form, with the increased *trans* content present in both crystallized and amorphous phases.

Density measurements have often been used to monitor changes in PET crystallinity, resulting from molecular orientation.^{1,7,26-28,30} Figure 3 shows that as uniaxial planar extension is increased, density also increases. As with the MD *trans* content seen in Figure 1, an increased rate of change occurs after extension ratios of 1 \times 2 have been achieved.

Birefringence is an additional means for measuring film anisotropy.^{24-28,31-33} Analyses were performed as described by Jabarin,²⁶ with birefringence (Δ) in each case calculated from refractive indices (n) taken for each of the three spatial directions:

$$\Delta_{\text{TD ND}} = n_{\text{TD}} - n_{\text{ND}}$$

$$\Delta_{\text{MD ND}} = n_{\text{MD}} - n_{\text{ND}}$$

$$\Delta_{\text{MD TD}} = n_{\text{MD}} - n_{\text{TD}}$$

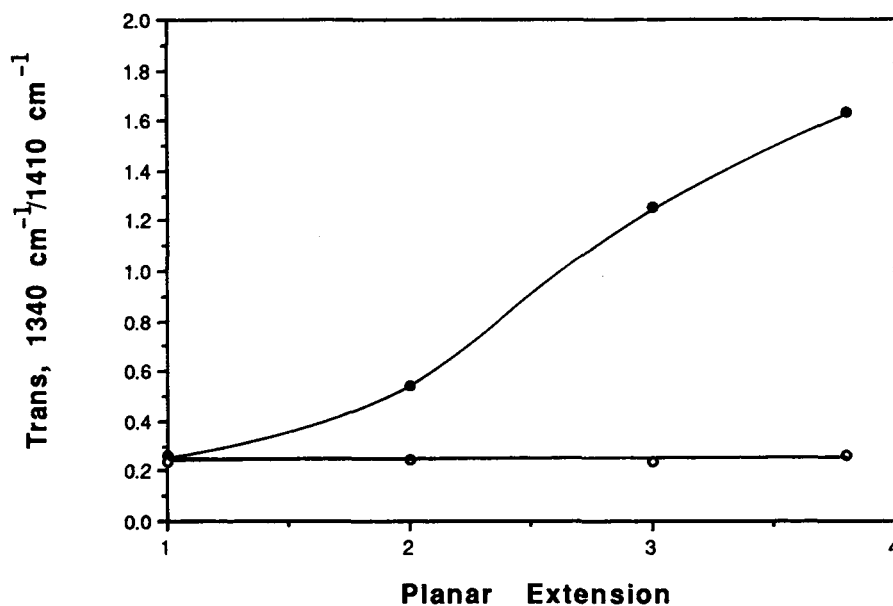


Figure 1 *Trans* conformation (normalized absorption at 1340 cm^{-1}) in relationship to uniaxial planar extension in the (●) MD and (○) TD.

Values calculated from refractive index measurements taken in all three film directions are shown in Figure 4 as functions of planar extension. Birefringence in the stretching direction (MD) is seen to exhibit a relationship to planar extension, similar to that observed for *trans* content and density in Figures 1 and 3, with the greatest rates of change noted for planar extensions greater than two. Con-

strained direction (TD) changes are much smaller than those obtained in the stretching direction, also consistent with infrared results.

Biaxial extension of PET films results in *trans* content variations similar to those observed for uniaxially extended, constrained films. Changes arising from biaxial stretching are shown in the following figures, as branches emanating from a major axis

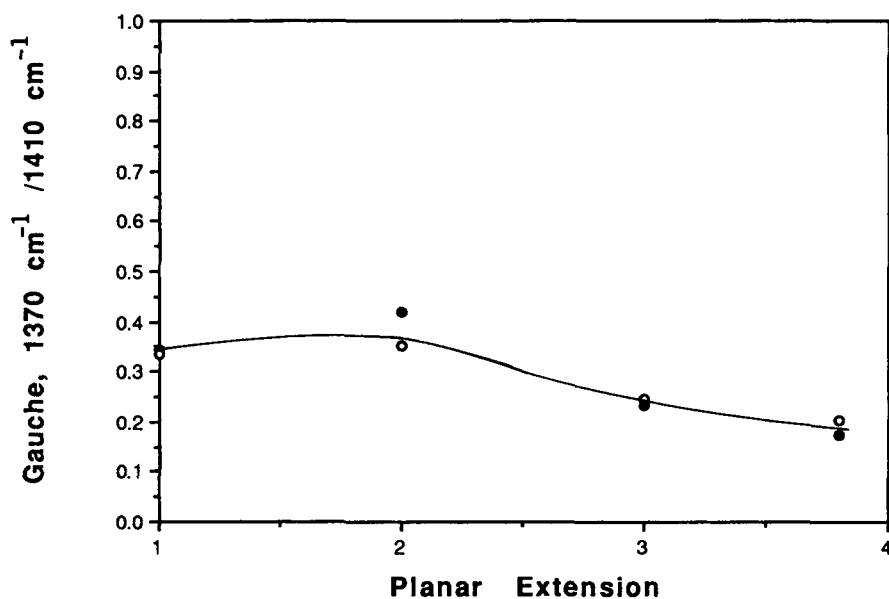


Figure 2 *Gauche* conformation (normalized absorption at 1370 cm^{-1}) in relationship to uniaxial planar extension in the (●) MD and (○) TD.

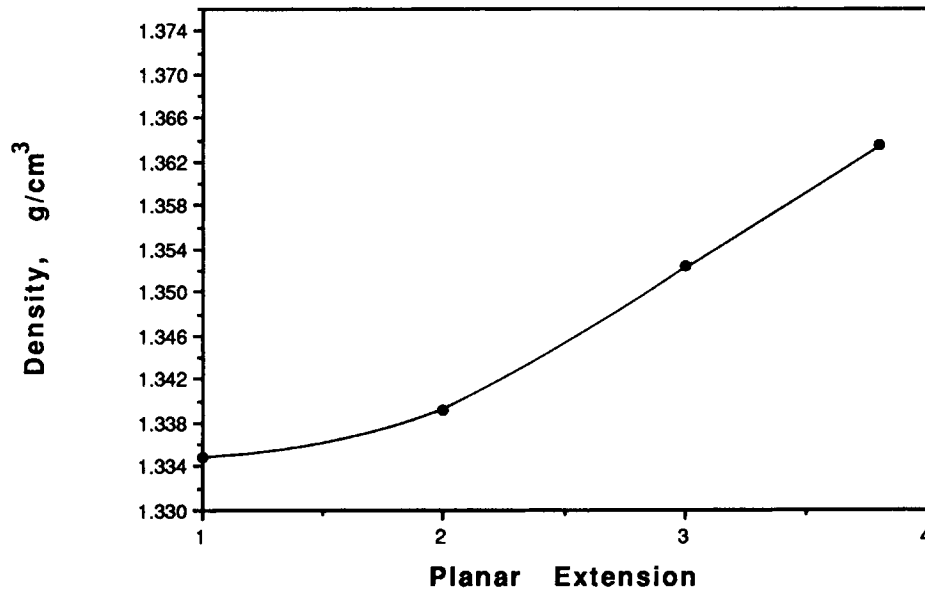


Figure 3 Density in relationship to uniaxial planar extension.

representing average values for samples unstretched and stretched equally in both directions. Data designated as MD has been measured in the greatest sample stretching direction (i.e., for 2×3 , in the 3 direction). Measurements performed in the lesser stretching direction (i.e., for 2×3 , in the 2 direction) are designated as TD.

Data shown in Figure 5 include the previously discussed uniaxially extended samples, a set of sam-

ples stretched 2×2 through 2×3.8 , and a set stretched 3×3 and 3×3.8 . In all cases, increased extension in the greatest stretching direction (MD) can be seen to result in increased *trans* content in this direction. Concurrent with these changes, values obtained in the lesser stretching direction (TD) for biaxially extended samples are seen to remain almost constant or decrease slightly with increased MD extension.

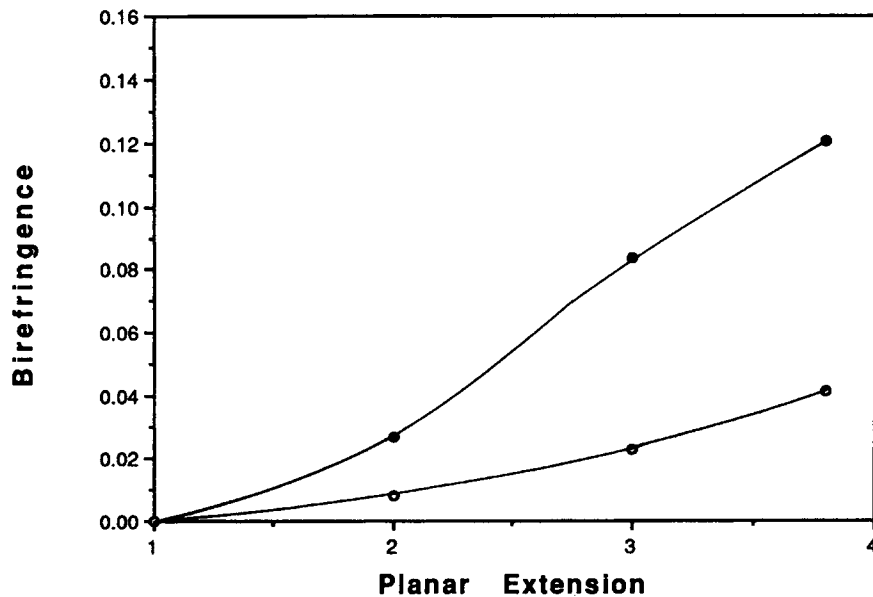


Figure 4 Birefringence in relationship to uniaxial planar extension in the (●) MD and (○) TD.

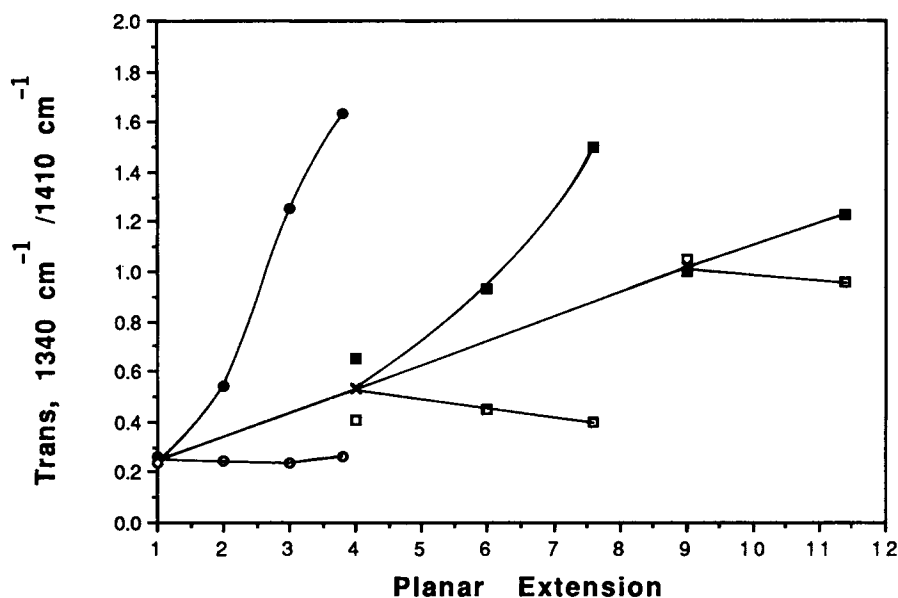


Figure 5 *Trans* conformation (normalized absorption at 1340 cm^{-1}) in relationship to planar extension for uniaxially stretched samples in the (●) MD and (○) TD as well as for biaxially stretched samples in the (■) MD and (□) TD. Average values for equal biaxially stretched samples are also shown (×).

The effects of molecular orientation upon *gauche* contents of PET films are shown in Figure 6. As previously discussed for uniaxially oriented films, *gauche* content is insensitive to orientation direction

and decreases steadily with increased planar extension.

Density increases resulting from increased planar extension are shown in Figure 7. Again, these values

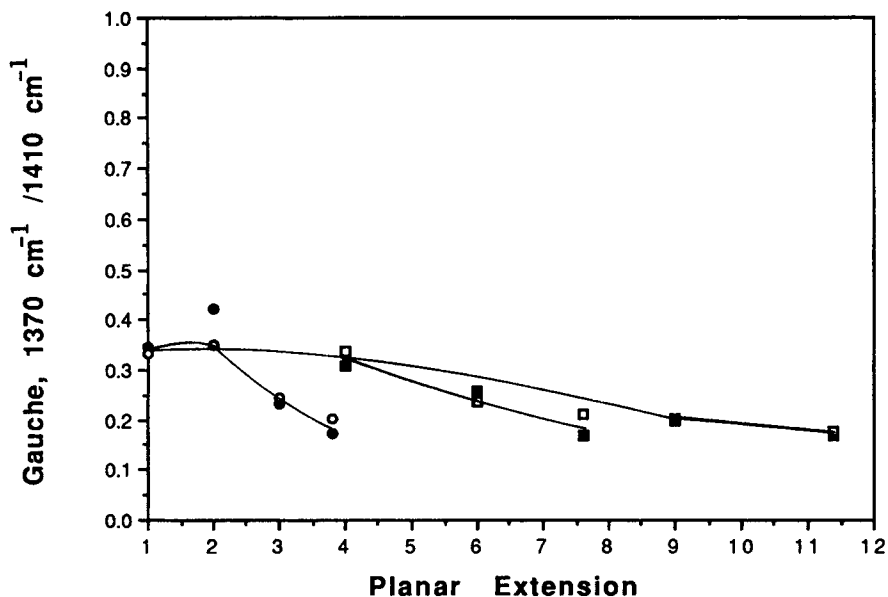


Figure 6 *Gauche* conformation (normalized absorption at 1370 cm^{-1}) in relationship to planar extension for uniaxially stretched samples in the (●) MD and (○) TD as well as for biaxially stretched samples in the (■) MD and (□) TD. Average values for equal biaxially stretched samples are also shown (×).

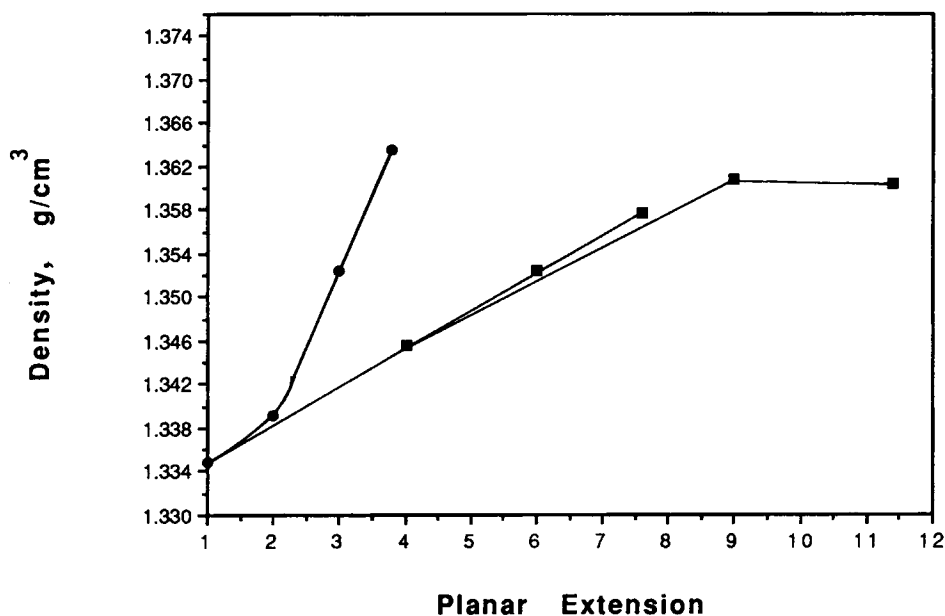


Figure 7 Density in relationship to (●) uniaxial and (■) biaxial planar extension.

follow the trends observed for *trans* values in the greater stretching directions, indicating increased crystallinity and orientation with greater extension ratios.

Birefringence is plotted as a function of planar extension in Figure 8. This plot is similar in shape to that observed for changes in *trans* content (Figure 5). As can be seen, the largest birefringence in-

creases are obtained in the direction of greatest sample orientation, with smaller increases seen in the lesser stretching direction. This is as expected, because both birefringence and *trans* contents are sensitive to orientation direction in the amorphous as well as in the crystalline phases of PET. As previously reported, uniaxially stretched samples exhibit greater changes in birefringence at lower planar

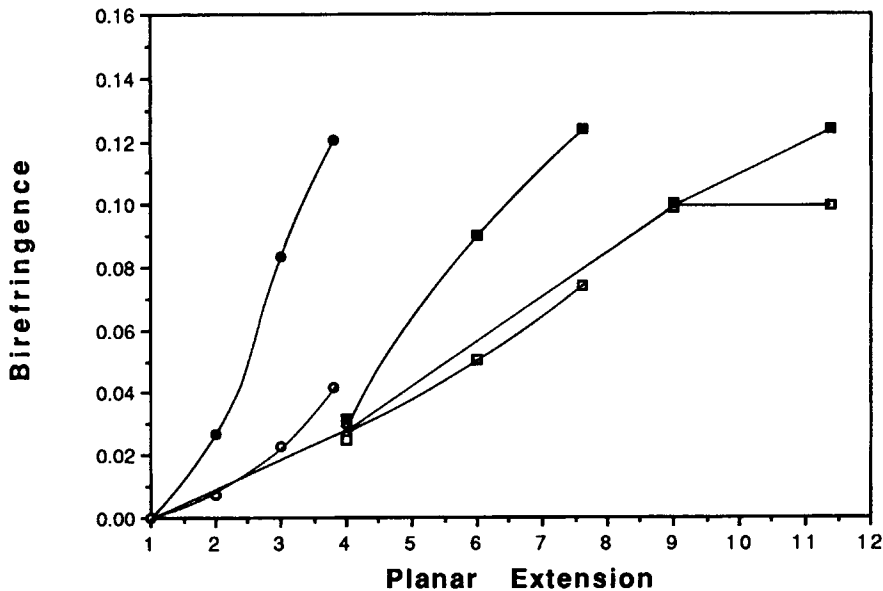


Figure 8 Birefringence in relationship to planar extension for uniaxially stretched samples in the (●) MD and (○) TD as well as for biaxially stretched samples in the (■) MD and (□) TD. Average values for equal biaxially stretched samples are also shown (×).

extensions than do biaxially oriented samples.²⁸ Similar results were noted for changes in density and MD *trans* contents.

The foregoing discussions have served to illustrate the utility of infrared IRS techniques for monitoring directional orientation of PET films. Additional results further substantiate the use of the specific measurement and reference bands chosen for this study.

In-plane-dichroism is taken as the ratio of normalized absorbance in the greatest stretching direction (MD) to that in the lesser stretching direction (TD) using only TE polarization waves (MD/TD). Such dichroic ratios should indicate the sensitivity of a given infrared band to orientation effects. Ideally, the *trans* band should show strong directional sensitivity, whereas the *gauche* and reference bands should be insensitive to such differences. It can be seen from the values on Tables I and II that the most consistent behavior is exhibited by the *trans* and *gauche* bands at 1340 and 1370 cm⁻¹, respectively. Figure 9 shows a comparison of dichroic ratios obtained for the three *trans* bands evaluated. It can be seen that dichroic ratios, calculated from normalized 1340 cm⁻¹ *trans* absorbance data, show continual increases with increased uniaxial and biaxial planar extensions. Results obtained using bands at 973 and 848 cm⁻¹ show expected behavior at moderate levels of uniaxial and biaxial planar extension.

As one direction of extension increases to higher levels, however, dichroic ratios taken at these wavenumbers decrease unexpectedly.

Dichroic ratios obtained using normalized *trans* and *gauche* bands from 1340 and 1370 cm⁻¹ measurements are shown in Figure 10 for uniaxially oriented samples. As expected, *trans* ratios increase with increased orientation, showing greater increases at planar extensions exceeding two. Ratios for *gauche* bands are about one, indicating the expected directional insensitivity of this measurement.

Results obtained for *trans* dichroic ratios calculated using values taken at 1340 cm⁻¹ are shown in Figure 11 for both uniaxially and biaxially oriented samples. As can be seen, results obtained for samples of equal biaxial extension are close to unity with greatest increases seen for the most unequally stretched samples. Results similar to those obtained for uniaxially oriented samples are shown in Figure 12 for the *gauche* (1320 cm⁻¹) ratios. As expected, these values are nearly one, indicating no significant orientation effects.

Equations for the determination of molecular orientation using IRS were first derived by Flournoy and Schaffers.¹⁸ They used Maxwell's field equations with the complex refractive indices to obtain reflectivity coefficients for thin surface layers of material. Others^{11,12,20-23} have reported further modifications and the use of these equations for calculation of

Table I. Normalized Absorption Values of Uniaxially Stretched Samples

Extension Ratio	Planar Extension	Measured Direction	<i>Trans</i> (cm ⁻¹)			<i>Gauche</i> (cm ⁻¹)		Reference (cm ⁻¹)	
			1340	973	848	1370	896	872	793
1 × 1	1	TD	0.238	0.286	0.479	0.333	0.809	1.844	0.711
		MD + ND	0.280	0.237	0.404	0.370	0.709	1.370	0.630
		MD	0.260	0.287	0.472	0.345	0.807	1.740	0.724
		TD + ND	0.297	0.247	0.409	0.388	0.726	1.371	0.653
1 × 2	2	TD	0.249	0.267	0.444	0.351	0.760	1.662	0.693
		MD + ND	0.329	0.242	0.364	0.381	0.649	1.268	0.606
		MD	0.541	0.474	0.639	0.421	0.993	1.684	0.993
		TD + ND	0.311	0.294	0.412	0.429	0.731	1.252	0.664
1 × 3	3	TD	0.238	0.265	0.504	0.244	0.492	1.605	0.440
		MD + TD	0.632	0.262	0.423	0.264	0.396	1.402	0.392
		MD	1.257	0.810	0.940	0.233	0.716	1.346	1.046
		TD + ND	0.243	0.196	0.421	0.267	0.484	1.714	0.447
1 × 3.8	3.8	TD	0.262	0.404	0.826	0.202	0.504	1.961	0.557
		MD + ND	0.908	0.325	0.482	0.215	0.382	1.974	0.412
		MD	1.639	0.453	0.534	0.172	0.315	0.636	1.070
		TD + ND	0.235	0.191	0.457	0.228	0.398	2.009	0.386

Peak distorted and band shifted at high extension ratios.

Table II. Normalized Absorption Values of Biaxially Stretched Samples

Extension Ratio	Planar Extension	Measured Direction	Trans (cm ⁻¹)			Gauche (cm ⁻¹)		Reference (cm ⁻¹)	
			1340	973	848	1370	896	872	793
2 × 2	4	TD	0.411	0.424	0.560	0.338	0.782	1.669	0.729
		MD + ND	0.354	0.248	0.402	0.341	0.608	1.338	0.527
		MD	0.652	0.674	0.729	0.307	0.861	1.684	0.819
2 × 3	6	TD + ND	0.373	0.242	0.432	0.331	0.598	1.526	0.522
		TD	0.449	0.551	0.748	0.236	0.685	1.816	0.654
		MD + ND	0.611	0.257	0.407	0.260	0.454	1.735	0.422
2 × 3.8	7.6	MD	0.933	1.103	1.053	0.258	0.908	1.982	1.032
		TD + ND	0.305	0.211	0.391	0.289	0.512	1.688	0.469
		TD	0.402	0.480	0.774	0.213	0.549	1.661	0.538
3 × 3	9	MD + TD	0.811	0.279	0.426	0.215	0.362	1.805	0.365
		MD	1.497	0.985	1.127	0.169	0.512	1.275	1.269
		TD + ND	0.326	0.181	0.403	0.219	0.361	1.952	0.358
3 × 3.8	11.4	TD	1.048	0.952	1.199	0.198	0.667	1.669	0.916
		MD + ND	0.611	0.255	0.418	0.243	0.389	1.858	0.380
		MD	1.002	0.858	1.078	0.201	0.642	1.556	0.875
3 × 3.8	11.4	TD + ND	0.617	0.261	0.428	0.233	0.404	1.829	0.395
		TD	0.959	0.837	1.079	0.177	0.250	1.421	0.796
		MD + ND	0.801	0.321	0.358	0.205	0.358	1.745	0.391
3 × 3.8	11.4	MD	1.230	0.561	0.799	0.168	0.402	0.951	0.844
		TD + ND	0.612	0.267	0.453	0.220	0.345	1.657	0.361

spatial attenuation indices (k_x , k_y , and k_z), which have been related to normalized absorption (A_{TE} and A_{TM}) values as follows:

Equations from Flournoy and Schaffers	Sample Direction Measured	
$A_{TE,x} = \alpha k_x$	TD	(1)
$A_{TM,x} = \beta k_y + \gamma k_z$	MD + ND	(2)
$A_{TE,y} = \alpha k_y$	MD	(3)
$A_{TM,y} = \beta k_x + \gamma k_z$	TD + ND	(4)

Values for the α , β , and γ constants were determined as follows²²:

$$\alpha = \frac{4n_{21}^2}{\tan \theta [1 - (n_{21}^2/\sin^2 \theta)]^{1/2} [1 - n_{21}^2]} \quad (5)$$

$$\beta = \frac{4n_{21}^2 [1 - (n_{21}^2/\sin^2 \theta)]}{\tan \theta [1 - (n_{21}^2/\sin^2 \theta)]^{1/2} \times [1 - (n_{21}^2/\sin^2 \theta) + n_{21}^4 \cot^2 \theta]} \quad (6)$$

$$\gamma = \frac{4n_{21}^2}{\tan \theta [1 - (n_{21}^2/\sin^2 \theta)]^{1/2} \times [1 - (n_{21}^2/\sin^2 \theta) + n_{21}^4 \cot^2 \theta]} \quad (7)$$

For these calculations, an average refractive index (n_2) of 1.6 was used for PET with an n_1 value of 2.38 for the KRS-5 element,^{1,18} giving an n_{21} value of 0.67. The angle of incidence, θ , was 45°. Values determined for α , β , and γ were, respectively, 10.64, 1.87, and 19.41.

Absorption values were obtained as previously described by orienting the x axis of the sample perpendicular and then parallel to the plane of incidence and, in each case, by setting the polarizer for both the TE and TM waves.^{21,22} Data obtained in each case were normalized with the reference band at 1410 cm⁻¹ to account for differences in sample contact, etc. These proportional values were then used with eqs. (1)–(4) to calculate the spatial attenuation indices.

Figure 13 gives the spatial attenuation indices obtained for uniaxially oriented samples. As can be seen, trends obtained in machine (k_y) and transverse (k_x) directions appear similar to those previously discussed for normalized absorption values (Fig. 1) and dichroic ratios (Fig. 10). Values obtained for k_z (ND) indicate a slight increase in planar orientation with increased planar extension.

Attenuation indices obtained for biaxially stretched samples are shown in Figure 14 along with those previously discussed for uniaxial samples. In

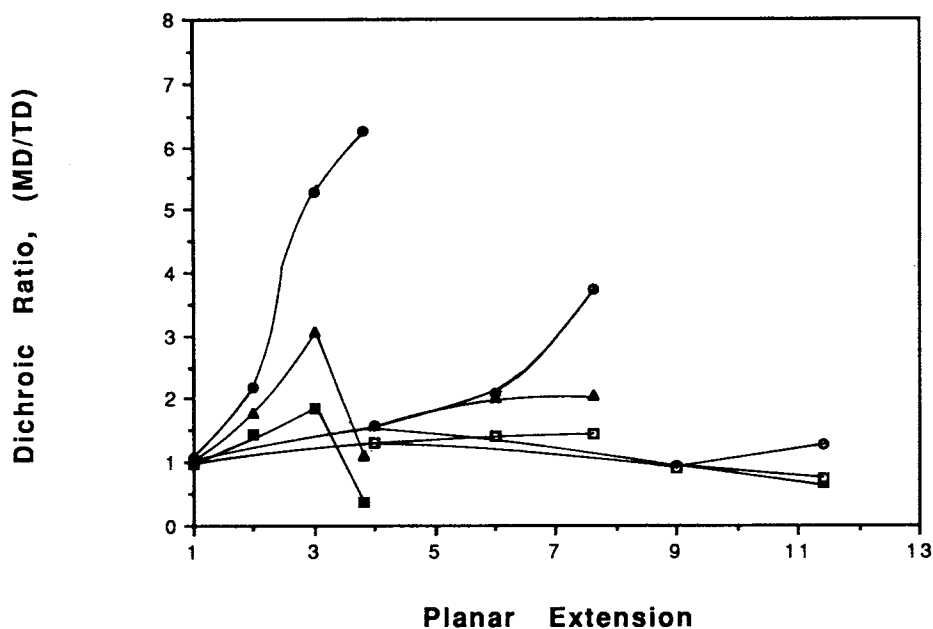


Figure 9 Dichroic ratios (MD/TD) in relationship to planar extension for uniaxially stretched samples at (●) 1340 cm^{-1} , (▲) 973 cm^{-1} , and (■) 848 cm^{-1} as well as for biaxially stretched samples at (○) 1340 cm^{-1} , (△) 973 cm^{-1} , and (□) 848 cm^{-1} .

this case, also, results obtained in the MD and TD directions (k_y and k_x) closely resemble those shown for absorption (Fig. 5) and dichroic ratio (Fig. 11). As with the uniaxial samples, planar orientation (\overline{kz}) is seen to increase steadily with increased

planar extension. This behavior is similar to directional sensitivity seen for birefringence and will be discussed in greater detail later.

The structural factor A_0 is independent of orientation and can be calculated using the three-

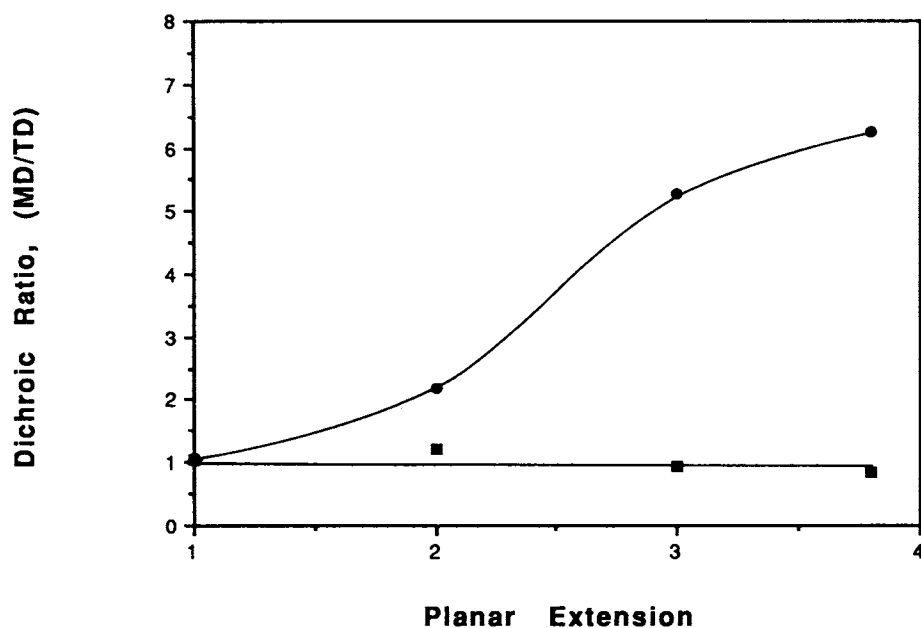


Figure 10 Dichroic ratios (MD/TD) in relationship to uniaxial planar extension for conformations of (●) *trans* at 1340 cm^{-1} and (■) *gauche* at 1370 cm^{-1} .

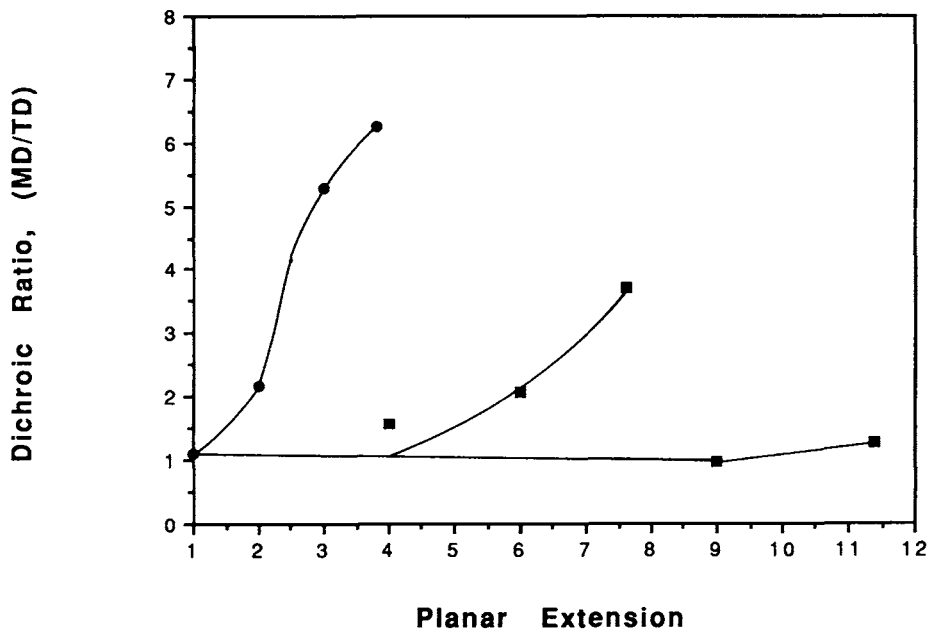


Figure 11 Dichroic ratios (MD/TD) in relationship to planar extension in terms of *trans* conformations at 1340 cm⁻¹ for (●) uniaxially and (■) biaxially stretched samples.

dimensional absorbance values as described by Schmidt¹:

$$A_0 = \frac{1}{3}(A_x + A_y + A_z) \quad (8)$$

Since the spatial attenuation indices obtained using eqs. (1)–(7) are proportional to A_x , A_y , and A_z ,

respectively, they can be substituted into eq. (8) to obtain a modified structural factor (A'_0):

$$A'_0 = \frac{1}{3}(k_x + k_y + \overline{kz}) \quad (9)$$

This modified factor should be proportional to the surface degree of crystallinity. Figure 15 shows A'_0

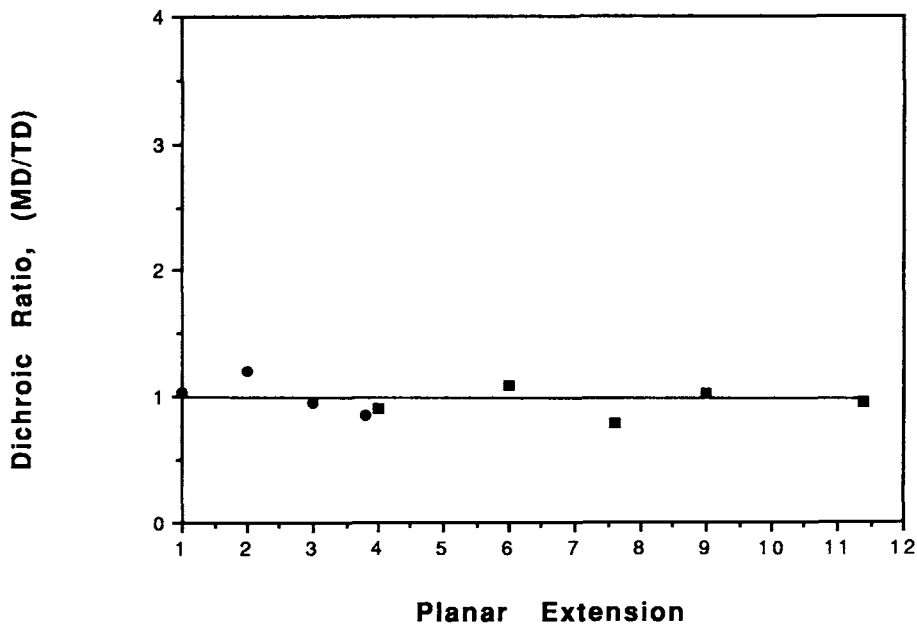


Figure 12 Dichroic ratios (MD/TD) in relationship to planar extension in terms of *gauche* conformations at 1370 cm⁻¹ for (●) uniaxially and (■) biaxially stretched samples.

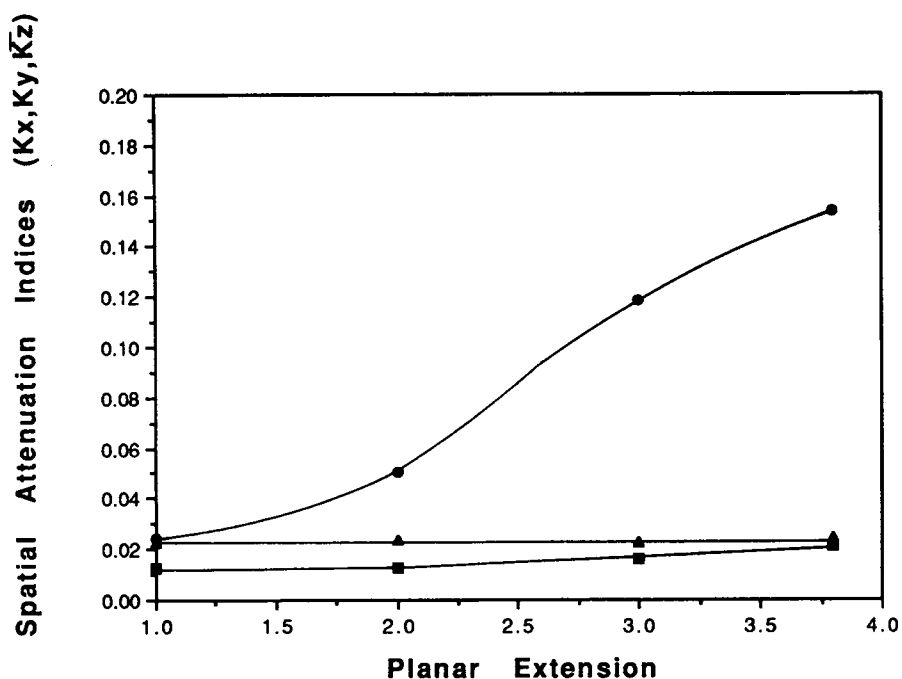


Figure 13 Spatial attenuation indices in relationship to uniaxial planar extension in ($k_y = \bullet$) machine, ($k_x = \blacktriangle$) transverse, and ($\bar{k}_z = \blacksquare$) normal directions.

values calculated for *gauche* and *trans* rotational isomers, plotted as functions of density or crystallinity. Calculations for volume fraction crystallinity

(V_c) are based on the relationship³³ $V_c = (d - d_a) / (d_c - d_a)$, in which d = sample density and d_a and d_c , respectively, represent amorphous (1.333 g/cm

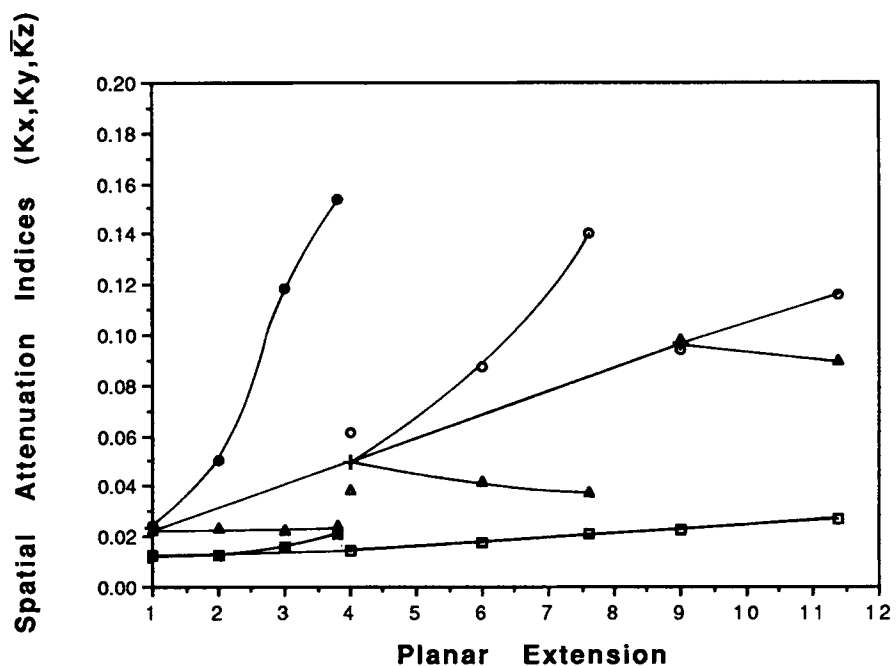


Figure 14 Spatial attenuation indices in relationship to planar extension for uniaxially stretched samples in ($k_y = \bullet$) machine, ($k_x = \blacktriangle$) transverse, and ($\bar{k}_z = \blacksquare$) normal directions as well as for biaxially stretched samples in ($k_y = \circ$) machine, ($k_x = \triangle$) transverse, and ($\bar{k}_z = \square$) normal directions.

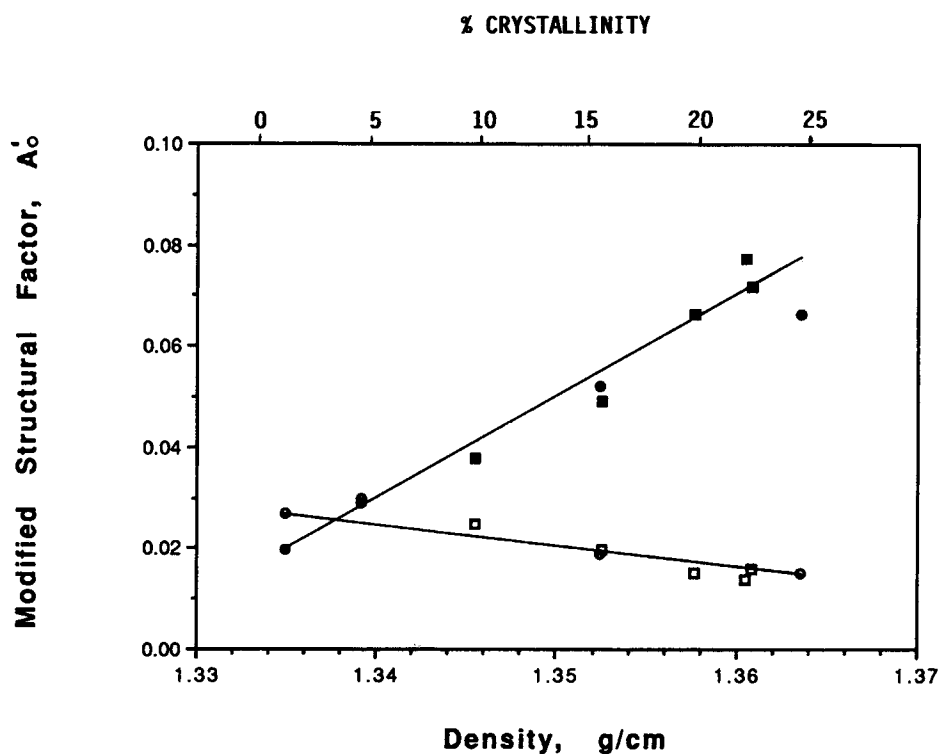


Figure 15 Modified structural factor A'_0 in relationship to sample density for the *trans* conformation at 1340 cm^{-1} of (●) uniaxially and (■) biaxially stretched samples. Relationships for the *gauche* conformation at 1370 cm^{-1} are also shown for (○) uniaxially and (□) biaxially stretched samples.

and crystalline (1.455 g/cm^3) densities⁷ of the PET homopolymer. As can be seen, rather good agreement has been achieved for the relationships among values obtained for density and modified structural factors. *Trans* values increase linearly with increased density, while the corresponding *gauche* values decrease. In addition, results obtained for samples oriented in both uniaxial and biaxial modes appear to exhibit equivalent relationships and fall on the same lines.

Segmental orientation has been determined by Fina and Koenig¹⁷ by ratioing absorption in each spatial direction (A_x , A_y , A_z) with the structural factor A_0 determined at the same wavenumber. Since values for k_x , k_y , and k_z [from eqs. (1)–(7)] are proportional to the spatial absorbance values and A_0 is proportional to the modified structural factor (A'_0) determined with eq. (9), similar relationships can be obtained for the IRS data. Figure 16 shows modified orientation parameters obtained for each spatial attenuation index ratioed with the modified structural factor (k_x/A'_0 , k_y/A'_0 , and k_z/A'_0). These results show relative orientation of *trans* rotational isomers in each of the three spatial direc-

tions. Similar relationships have been established by Samuels³³ using refractive index values. In this case, the average refractive index (\bar{N}) is calculated for refractive indices in each of the spatial directions as follows:

$$\bar{N} = \frac{1}{3}(n_x + n_y + \bar{n}_z) \quad (10)$$

Individual refractive index values, measured in each spatial direction, can then be ratioed with \bar{N} to obtain refractive index orientation parameters. These results are shown in Figure 17. As can be seen, orientation relationships in each spatial direction (TD, MD, and ND) are similar for results obtained using IRS and refractive index techniques.

Herman's orientation function (f) may be calculated from dichroic ratios (D) obtained as follows^{12,22,23}:

$$f = \frac{(D - 1)(D_0 + 2)}{(D + 2)(D_0 - 1)} \quad (11)$$

where $D_0 = 2 \cot^2 \alpha$, and α is the angle between the transition moment vector for the vibration and the

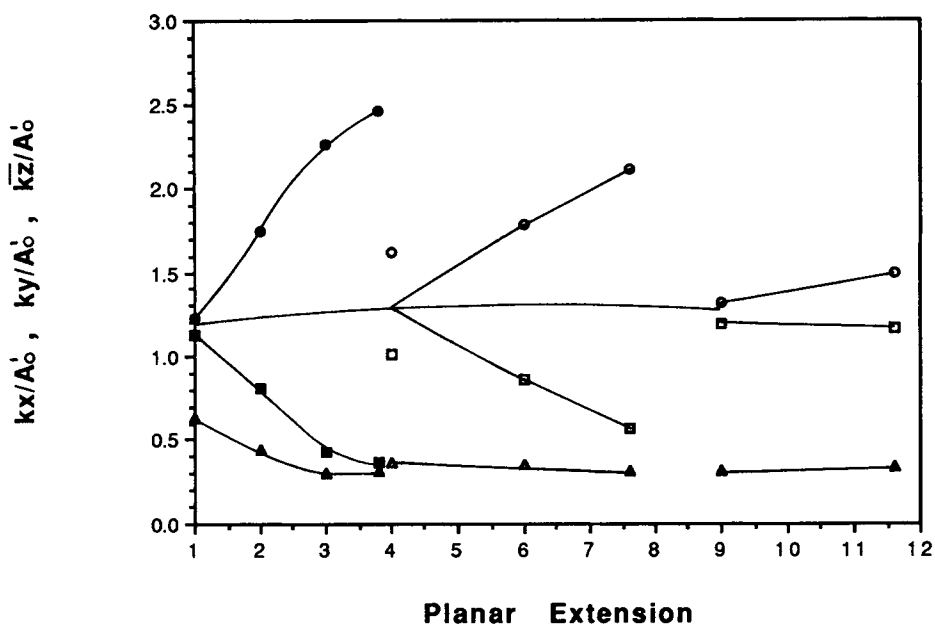


Figure 16 Modified segmental orientation parameters in relationship to planar extension for uniaxially stretched samples in the ($ky/A'_0 = \bullet$) machine, ($kx/A'_0 = \blacksquare$) transverse, and ($\bar{kz}/A'_0 = \blacktriangle$) normal directions. Values for biaxially stretched samples are shown in the ($ky/A'_0 = \circ$) machine, ($kx/A'_0 = \square$) transverse, and ($\bar{kz}/A'_0 = \triangle$) normal directions.

chain axis.¹² If perfect alignment with the stretching direction has been achieved, $f = 1$. If alignment is random, $f = 0$, and if transverse, $f = -0.5$.

For the special case where the transition moment is approximately parallel to the chain axis (i.e., α approaches 0), the orientation function f may be

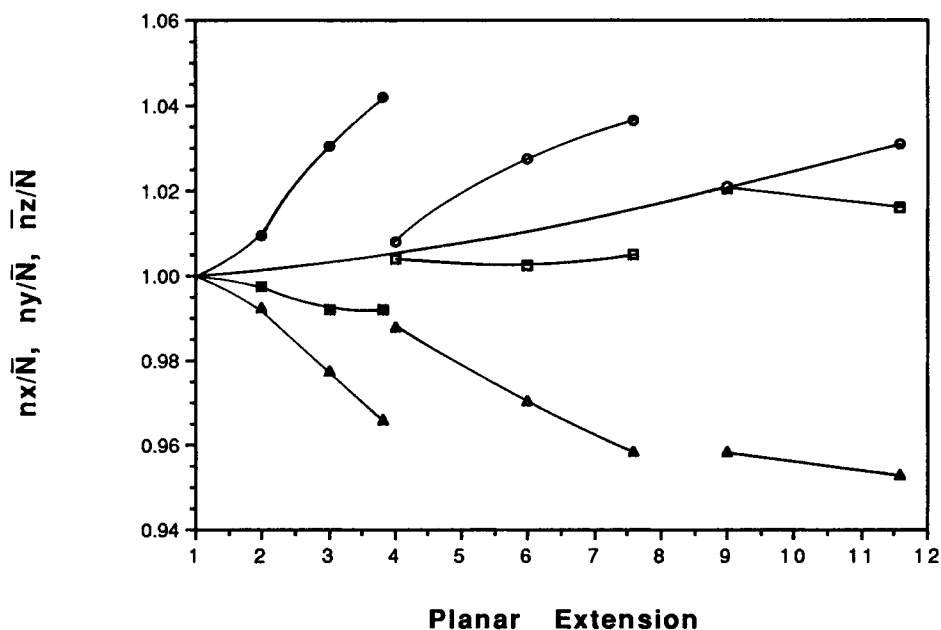


Figure 17 Refractive index orientation parameters in relationship to planar extension for uniaxially stretched samples in the ($ny/\bar{N} = \bullet$) machine, ($ny/\bar{N} = \blacksquare$) transverse, and ($\bar{nz}/\bar{N} = \blacktriangle$) normal directions. Values for biaxially stretched samples are shown in the ($ny/\bar{N} = \circ$) machine, ($nx/\bar{N} = \square$) transverse, and ($\bar{nz}/\bar{N} = \triangle$) normal directions.

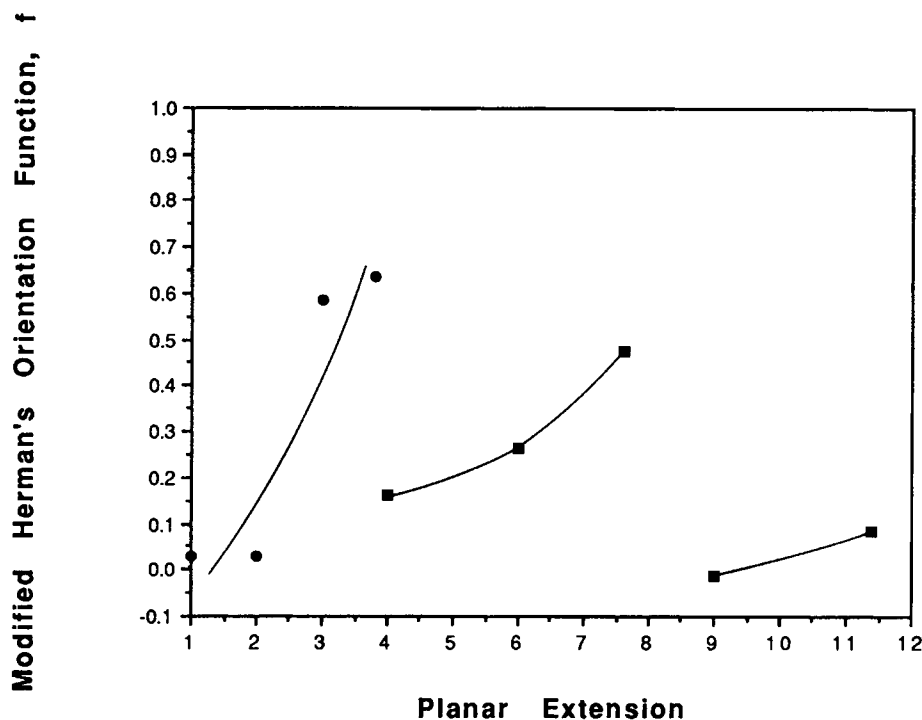


Figure 18 Modified Herman's orientation function in relationship to planar extension for (●) uniaxially and (■) biaxially stretched samples.

calculated as follows³⁴:

$$f = \frac{(D - 1)}{(D + 2)} \quad (12)$$

As an approximation, minimum values of f can be calculated using eq. (12), with the assumption that $\alpha = 0$.¹² Figure 18 shows these estimated orientation functions, plotted vs. planar extension. It can be seen that values for f increase most readily as extension ratios are increased for samples stretched in the uniaxially constrained mode. Alignment in the plane of the film is more random for the biaxially stretched samples, as would be expected. Biaxially stretched samples, with TD stretch ratios of 2 and MD ratios of 2 and above, show higher values for f than those with stretch ratios of 3×3 and above. In all cases, as MD stretch ratios exceed TD ratios by greater amounts, orientation functions increase accordingly.

CONCLUSIONS

Changes in molecular orientation and crystallinity of PET film surfaces have been successfully evalu-

ated utilizing polarized internal reflectance spectroscopy (IRS). Measurements were performed on samples stretched in both uniaxial and biaxial modes. A reference band at 1410 cm^{-1} , resulting from phenylene ring vibrations, was used to normalize all other bands of interest. Most consistent results were obtained with *gauche* and *trans* rotational isomers of the ethylene glycol linkages, present at 1370 and 1340 cm^{-1} , respectively.

Use of the 1410 cm^{-1} reference band for normalizing individual spectra overcomes most problems associated with variations in effective sample thickness and makes the IRS technique much more useful for measuring orientational changes in PET.

Infrared data were found to show good agreement with values obtained using density and refractive index measurements. Orientation parameters have been calculated in the three spatial directions and found to correspond to similar normalized refractive index measurements. Modified structural factors obtained from changes in *gauche* and *trans* bands were found to relate linearly to density changes, within the investigated range. Orientation functions, calculated from dichroic ratios in the MD vs. TD directions, increased as expected for each orientation condition.

REFERENCES

1. P. G. Schmidt, *J. Polym. Sci. A-1*, 1271 (1963).
2. C. J. Heffelfinger and P. G. Schmidt, *J. Appl. Polym. Sci.*, **9**, 2661 (1965).
3. R. G. J. Miller and H. A. Willis, *J. Polym. Sci. C*, **19**, 485 (1956).
4. J. L. Koenig and S. W. Cornell, *J. Polym. Sci. C*, **22**, 1019 (1969).
5. G. Farrow and I. M. Ward, *Polymer*, **1**, 330 (1960).
6. M. Ito, J. R. C. Pereira, and R. S. Porter, *J. Polym. Sci. Polym. Lett.*, **20**, 61 (1982).
7. M. Ito, J. R. C. Pereira, S. L. Hsu, and R. S. Porter, *J. Polym. Sci. Polym. Phys. Ed.*, **21**, 389 (1983).
8. A. Miyake, *J. Polym. Sci.*, **38**, 479 (1959).
9. I. J. Hutchinson, I. M. Ward, H. A. Willis, and V. Zichy, *Polymer*, **21**, 55 (1980).
10. D. A. Jarvis, I. J. Hutchinson, D. I. Bower, and I. M. Ward, *Polymer*, **21**, 41 (1980).
11. C. S. P. Sung and J. P. Hobbs, *Chem. Eng. Commun.*, **30**, 229 (1984).
12. J. P. Hobbs, C. S. P. Sung, K. Krishnan, and S. Hill, *Macromolecules*, **16**(2) 193 (1983).
13. D. J. Walls, *Appl. Spectrosc.*, **45**(7), 1193 (1991).
14. J. L. Koenig, *Spectroscopy of Polymers*, American Chemical Society, Washington, DC, 1991, Chap. 4.
15. S. B. Lin and J. L. Koenig, *J. Polym. Sci. Polym. Phys.*, **20**, 2277 (1982).
16. L. J. Fina and J. L. Koenig, *J. Polym. Sci. Part B Polym. Phys.*, **24**, 2509 (1986).
17. L. J. Fina and J. L. Koenig, *J. Polym. Sci. Part B Polym. Phys.*, **24**, 2525 (1986).
18. P. A. Flournoy and W. J. Schaffers, *Spectrochim. Acta*, **22**, 5 (1966).
19. P. A. Flournoy, *Spectrochim. Acta*, **22**, 15 (1966).
20. N. J. Harrick, *Internal Reflection Spectroscopy*, Wiley-Interscience Wiley, New York, 1967.
21. F. M. Mirabella, Jr. and N. J. Karrick, *Internal Reflection Spectroscopy: Review and Supplement*, Marcel Dekker, New York, 1985.
22. F. M. Mirabella, Jr., *Internal Reflection Spectroscopy: Theory and Applications*, Marcel Dekker, New York, 1993.
23. F. M. Mirabella, Jr., *Appl. Spectrosc.*, **42**(7), 1258 (1988).
24. S. Okajima, Y. Koizumi, and K. Kagakyu, *Zusshi*, **42**, 810 (1939).
25. G. W. Schael, *J. Appl. Polym. Sci.*, **8**, 2717 (1964).
26. S. A. Jabarin, *Polym. Eng. Sci.*, **24**(5), 376 (1984).
27. S. A. Jabarin, *Polym. Eng. Sci.*, **32**(18), 1341 (1992).
28. P. Chandran and S. Jabarin, *Adv. Polym. Technol.*, **12**(2), 153 (1993).
29. P. Chandran and S. Jabarin, *Adv. Polym. Technol.*, **12**(2), 119 (1993).
30. P. Chandran and S. Jabarin, *Adv. Polym. Technol.*, **12**(2), 133 (1993).
31. M. Cakmak, J. L. White, and J. E. Spruiell, *Polym. Eng. Sci.*, **29**(21), 1534 (1989).
32. M. Cakmak, J. E. Spruiell, and J. L. White, *Polym. Eng. Sci.*, **24**(18), 1390 (1984).
33. R. J. Samuels, *J. Appl. Polym. Sci.*, **26**, 1383 (1981).
34. B. E. Read, in *Structure and Properties of Oriented Polymers*, I. M. Ward, Ed., Wiley, New York, 1975.

Received May 24, 1993

Accepted August 9, 1993